

Improvements and Corrections to AT123D Code

by Daniel K. Burnell¹, Barry H. Lester², and James W. Mercer³

Abstract

Although based on exact analytical solutions, semi-analytical solute transport models can have significant numerical error in applications with high frequency oscillatory source terms and when parameter value combinations cause series solution approximations to converge slowly. Methods for correcting these numerical errors are presented and implemented in the AT123D code, which employs Green's functions to represent point, linear, and rectangular prismatic source zones. In order to increase its computational accuracy, a Romberg numerical integration scheme was added to AT123D with prespecified error criteria, variable time stepping, and partitioning of the integral to handle rapidly changing source terms. More rapidly converging series solution approximations for the Green's functions were also incorporated to improve both accuracy and computational efficiency for finite-depth aquifers. AT123D also has been modified to eliminate redundant calculations at points where approximate steady-state conditions have been reached to improve computational efficiency during numerical integration. These modifications help to decrease computer run times that can be excessive for three-dimensional problems with large numbers of computational points, small time steps, and/or long simulation time periods. Errors in the original AT123D code also were corrected in this modified version, AT123D-AT, in order to accurately simulate finite-duration (pulse) source releases.

Introduction

The use of Green's functions in semi-analytical models such as AT123D (Yeh 1981, 1993) provides a flexible means to simulate the advective-dispersive transport of chemicals, radionuclides, and heat from a wide variety of source configurations in aquifers bounded by various boundary conditions. This approach combines the product of solutions of point and/or integrated line sources in each of the three principal directions. With an appropriate numerical integration technique, the Green's function approach provides accurate solution of advective-dispersive transport with first-order decay from a point,

line, rectangular planar, or rectangular prismatic source (Figure 1). In AT123D, the modeled aquifer is considered to be infinite in the horizontal direction of flow, but can be simulated as finite or infinite in both the horizontal and vertical transverse directions (Figure 2). The source release may be instantaneous, steady (finite or infinite in length), or variable over time. The versatility of the model is demonstrated by numerous source and aquifer configurations, and the time-variant source options that are available.

The AT123D model has been used to simulate three-dimensional (3D) dissolved chemical transport in groundwater in a variety of hydrogeologic settings (Water Resources Control Board [WRCB] 1989; Duffield and GeoTrans 1996; Sinton et al. 2000; King and Geo 2006). In addition to its use as a stand-alone model, AT123D is often used in conjunction with vadose zone exposure assessment models such as the integrated screening-level soil compartment model SESOIL (Bonazountas and Wagner 1984; WRCB 1989; Odencrantz et al. 1992; Hetrick et al. 1989, 1993; General Sciences Corporation, 1995), one-dimensional (1D) finite-difference vadose zone

¹Corresponding author: Tetra Tech GEO, Inc., 21335 Signal Hill Plaza Suite 100, Sterling, VA 20164; (703) 885-5438; fax: (703) 444-1685; dan.burnell@tetratech.com

²Tetra Tech GEO, Inc., 205 Cody Lane Apt. 5, Aiken, SC 29803.

³Tetra Tech GEO, Inc., 21335 Signal Hill Plaza Suite 100, Sterling, VA 20164.

Received September 2011, accepted December 2011.

© 2012, The Author(s)

Ground Water © 2012, National Ground Water Association.

doi: 10.1111/j.1745-6584.2011.00905.x

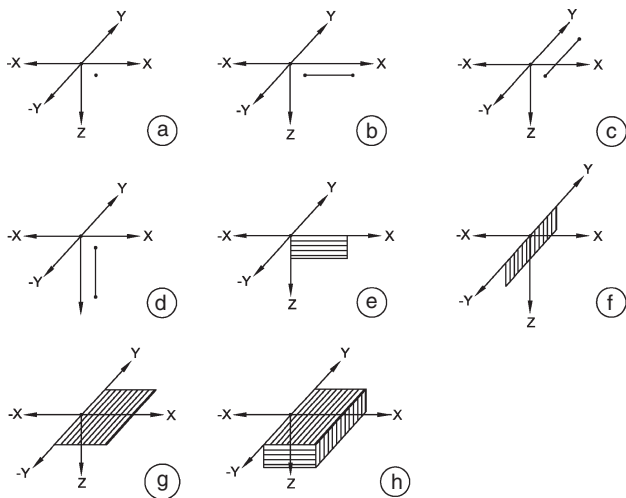


Figure 1. Source configurations in AT123D-AT based upon the combination of one-dimensional Green's functions.

leaching model VLEACH (United States Environmental Protection Agency [USEPA] 1996), and the screening model JURY (Jury et al. 1990), which estimates chemical flux and volatilization within the vadose zone. AT123D is also used in both the American Petroleum Industry's Decision Support System (DSS) for exposure and risk assessment (American Petroleum Institute [API] 1994) and SEVIEW (Environmental Consultants Inc. 2006) fate and transport modeling interface. Some states specify the use of AT123D to examine impacts to groundwater from soil contamination including New Jersey, which has a guidance document regarding its use (New Jersey Department of Environmental Protection [NJDEP] 2008).

Because AT123D is based on an exact analytical solution, its analytical solutions are not subject to the significant errors (West et al. 2007) that can occur in codes such as BIOCHLOR and BIOSCREEN (Newell et al. 1996; Aziz et al. 2000), which incorporate the Domenico (1987) solution, and introduce mathematical error when the specified value for the longitudinal dispersion coefficient is nonzero (Srinivasan et al. 2007; Burnell et al. 2011).

Although they are based on exact analytical solutions, semi-analytical models, including the original version of AT123D (Yeh 1981), can have difficulties in numerical accuracy. These difficulties can originate from: (1) the use of too coarse of a time step (or more accurately, time-integration partition) in the numerical integration scheme; and (2) the need for additional series terms in evaluating finite-width and finite-depth aquifers. In addition, computer run times requiring sufficient accuracy can be excessive in semi-analytical models in 3D problems where there is a large number of computational points, small time steps, and/or long simulation time periods. Although AT123D performed well in various code comparisons with MODFLOW/MT3D (Cecan and Schneiber 2010), incorrect answers in AT123D can arise from the use of the pulse-source option, which is incorrectly coded in the original version.

In this paper, methods for correcting these problems in semi-analytical models are presented and implemented through modifications of the numerical methods in AT123D into its updated version AT123D-AT. This paper first provides a description of AT123D-AT including the governing equations and general solution. The Green's functions used in AT123D-AT are discussed with a focus on the new series approximations that are used to

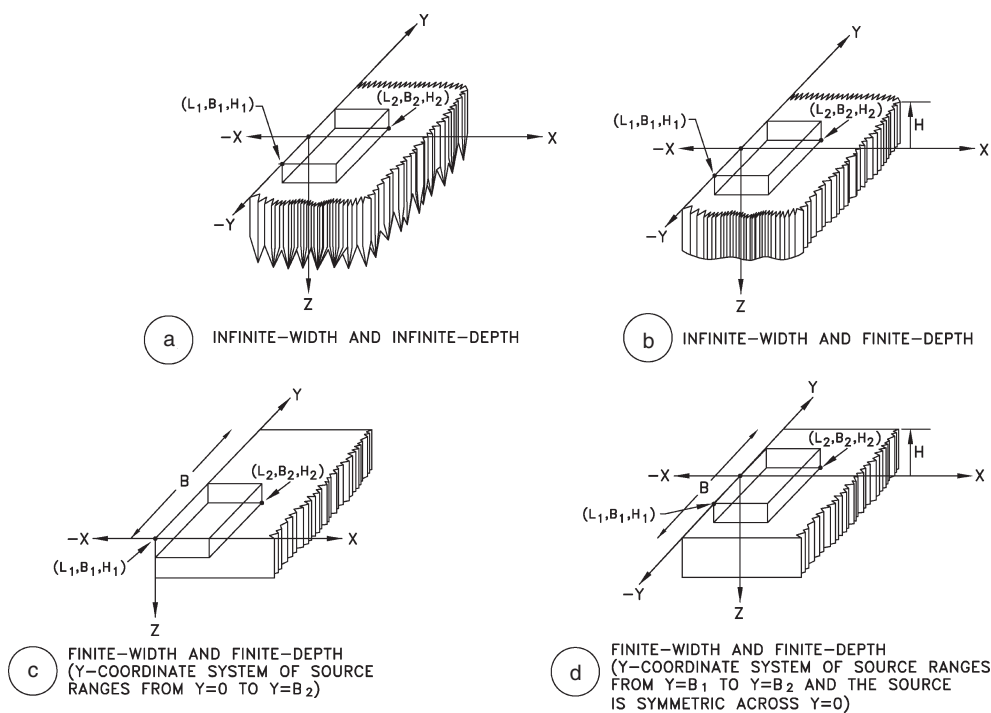


Figure 2. Various aquifer geometries used in AT123D-AT.

increase convergence rates and computational accuracy in analytical solutions for aquifers with finite thickness. Methods for representing both unsaturated and saturated source zones are then presented. Finally, the use of a more robust Romberg numerical integration scheme in AT123D-AT that generates accurate solutions regardless of the time steps and evaluation points that are chosen is discussed. Two example simulations are considered. The first example simulation is for a finite-duration (pulse) source in order to examine code corrections of an error found in the original AT123D code. The second example simulation examines the accuracy of new numerical integration and series solution approximations in AT123D-AT through the comparison of results with a numerical model.

Model Description

The original AT123D model is described by Yeh (1981). The analytical solutions in AT123D and its updated version AT123D-AT describe the advective-dispersive transport of dissolved species in an aquifer that can be approximated as a porous medium. The groundwater flow field is considered to be uniform, both spatially and temporally. Aquifer boundaries are assumed to be infinite in the direction of flow (along the x axis), with options of infinite- or finite-width boundaries in the horizontal plane, and semi-infinite- or finite-depth boundaries in the vertical plane parallel to flow (Figure 2). The coordinate system for the finite-width aquifer option in the original version of AT123D is based on the coordinate system starting at $y = 0$ and ending at $y = B$, where B is the width of the aquifer (Figure 2c). AT123D-AT has a new option that allows the user to choose the y coordinates of the finite aquifer to extend from $y = -B/2$ to $y = B/2$ (Figure 2d) for an aquifer of width B .

Conceptually, the upper boundary of the vertical plane ($z = 0$) represents the water table or top of a confined or semi-confined aquifer. At an initial time, the water in the aquifer starts out as clean, and mass of dissolvable material is added to the system. The source term, which represents the mass added, may be used to simulate: (1) dissolved and sorbed mass-in-place in the saturated zone; (2) mass entering the dissolved phase at solubility limits from a nonaqueous phase liquid (NAPL) source; or (3) mass entering the aquifer due to either leaching from the vadose zone, an overlying landfill, or leakage from an overlying aquifer/aquitard system. In the AT123D analytical solutions, the mass added is immediately partitioned into dissolved and sorbed phases, which are assumed to decay at the same rate.

Governing Equations

Based on this conceptual model, the 3D advection-dispersion equation with linear sorption and first-order

degradation in AT123D is

$$n_e R \frac{\partial C}{\partial t} = D_{xx} \frac{\partial^2 C}{\partial x^2} + D_{yy} \frac{\partial^2 C}{\partial y^2} + D_{zz} \frac{\partial^2 C}{\partial z^2} - q \frac{\partial C}{\partial x} - n_e R \lambda C + \dot{M} \quad (1a)$$

where C is the concentration of the dissolved species, q the Darcy velocity, n_e the effective porosity, D_{xx} , D_{yy} , and D_{zz} the principal values of the hydrodynamic dispersion tensor aligned in the x -, y -, and z -coordinate directions, t the time, λ the first-order decay constant, $\dot{M}(x, y, z, t)$ the rate of mass released from the user-defined source configuration during the period of activity, and R the retardation factor.

For an aquifer with finite width and depth, the initial and boundary conditions in AT123D are

$$C(x, y, z, 0) = 0 \quad (1b)$$

$$C(x, y, z, t) \rightarrow 0 \quad \text{as } x \rightarrow \pm\infty \quad (1c)$$

$$D_y \frac{\partial C}{\partial y} = 0 \quad \text{at } y = -\frac{B}{2} \text{ and } y = \frac{B}{2} \quad (1d)$$

$$D_z \frac{\partial C}{\partial z} = 0 \quad \text{at } z = 0 \text{ and } z = H \quad (1e)$$

where B is the aquifer width (y direction) and H the aquifer thickness (z direction). When the contaminant extent is much less than the width or depth of the aquifer, AT123D can also utilize the following infinite boundary conditions for aquifers of large width and thickness:

$$C \rightarrow 0 \text{ as } y \rightarrow \pm\infty \quad (1f)$$

$$C \rightarrow 0 \text{ as } z \rightarrow \infty \quad (1g)$$

General Solution

For simple source geometries (Figure 1) that can be described by separate coordinate directions, Yeh (1981) derived the solution to Equation 1a subject to the initial condition (Equation 1b) and either no-flux boundary conditions (Equations 1c to 1e) or infinite boundary conditions (Equation 1f to 1g) by constructing Green's functions in a manner analogous to that used in potential theory (e.g., Kellogg 1955; Carslaw and Jaeger 1959). The 3D solution can be written in the form:

$$C(x, y, z, t) = \int_0^t \iiint_{R'} \frac{\dot{M}(x_0, y_0, z_0, t_0)}{n_e R} \times G(x, y, z, t; x_0, y_0, z_0, t_0) \times dx_0, dy_0, dz_0, dt_0 \quad (2)$$

where R' is the space occupied by the source and G the Green's function solution for the response at (x, y, z) due

to a point source at (x_0, y_0, z_0) acting instantaneously at time t_0 (Haberman 1987). For source configurations such as Figure 1, the Green's function can be expressed as

$$G(x, y, z, t; x_0, y_0, z_0, t_0) = G_x(x, t; x_0, t_0)G_y(y, t; y_0, t_0)G_z(z, t; z_0, t_0) \quad (3)$$

(Carslaw and Jaeger 1959) where the three basic response functions $G_x(x, t; x_0, t_0)$, $G_y(y, t; y_0, t_0)$, and $G_z(z, t; z_0, t_0)$ for each respective 1D equation can be written in the form:

$$G_x = \frac{1}{\sqrt{4\pi D'_{xx}(t-t_0)}} \times \exp\left[-\frac{\{(x-x_0)-v'(t-t_0)\}^2}{4D'_{xx}(t-t_0)} - \lambda(t-t_0)\right] \quad (4a)$$

$$G_y = \frac{1}{\sqrt{4\pi D'_{yy}(t-t_0)}} \exp\left[-\frac{(y-y_0)^2}{4D'_{yy}(t-t_0)}\right] \quad (4b)$$

$$G_z = \frac{1}{\sqrt{4\pi D'_{zz}(t-t_0)}} \exp\left[-\frac{(z-z_0)^2}{4D'_{zz}(t-t_0)}\right] \quad (4c)$$

where v' is the retarded seepage velocity, defined as $v' = q/(n_e R)$, and $(t-t_0)$ the time elapsed since the point source at location (x_0, y_0, z_0) is applied. The dispersion coefficients have been redefined for convenience based upon the retarded seepage velocity, so that $D'_{ii} = (a_{ii}q + D_{\text{eff}})/(n_e R)$, where a_{ii} are the x , y , and z -direction principal values of the dispersivity tensor and D_{eff} is the effective diffusion coefficient. Equation 4a is the solution for an instantaneous point source at time t_0 at location x_0 with unidirectional flow in the x direction and first-order decay in an infinite 1D medium. Equations 4b and 4c are the infinite 1D solutions for an instantaneous point-source release at time t_0 at point y_0 in the y direction and point z_0 in the z direction, respectively (Carslaw and Jaeger 1959).

The general solution (Yeh 1981) of Equation 1 for the advective-dispersive transport of a dissolved species in groundwater can be written as follows. For a continuous source release of finite duration (T) and time $t < T$:

$$C(x, y, z, t) = \int_0^t \frac{\dot{M}(t_0)}{n_e R} F_{ijk}(x, y, z, t; t_0) dt_0. \quad (5a)$$

For a finite-duration source and time $t > T$

$$C(x, y, z, t) = \int_0^T \frac{\dot{M}(t_0)}{n_e R} F_{ijk}(x, y, z, t; t_0) dt_0. \quad (5b)$$

For an instantaneous source:

$$C(x, y, z, t) = \frac{M}{n_e R} F_{ijk}(x, y, z, t; t_0 = 0) \quad (5c)$$

where the term F_{ijk} is the integral of Green's function G over the source space, M the mass released over the

defined source configuration, and T the duration of waste release. The influence function F_{ijk} is defined as

$$F_{ijk} = X_i Y_j Z_k \quad (6)$$

where X_i , Y_j , and Z_k are the basic or spatially integrated Green's functions in the x -, y -, and z - directions, respectively. The indices $i = 1$ or 2 , $j = 1, 2, 3, 4, 5$, or 6 , and $k = 1, 2, 3, 4, 5$, or 6 denote the specific Green's functions available in AT123D-AT for each principal coordinate direction as presented below.

Green's Functions in AT123D-AT

The power of Green's functions is their applicability to represent a wide range of source configurations (Figure 1) and releases including steady, pulse, and transient. Superposition of Green's functions allows for the simulation of one or more sources that operate at different times. Spatial integration of the basic Green's functions allows for the development of solutions for various source configurations, and temporal integration allows for the analysis of the influence of transient sources. By considering only relatively simple source geometries, such as point, line, rectangular, and rectangular prismatic, where all forms are oriented parallel or perpendicular to the coordinate axes, the necessary Green's functions in AT123D and AT123D-AT can be developed analytically by integrating the basic functions over the spatial domain. These Green's functions are derived below with a discussion of updates in AT123D-AT that improve the convergence rates of the series approximations for finite-depth aquifers.

x Direction

The Green's functions available in AT123D-AT for advective-dispersive transport in the flow direction from a point source is

$$X_1 = \frac{1}{\sqrt{4\pi D'_{xx}(t-t_0)}} \times \exp\left[-\frac{\{(x-x_0)-v'(t-t_0)\}^2}{4D'_{xx}(t-t_0)} - \lambda(t-t_0)\right] \quad (7)$$

where x_0 is the x coordinate of the point source. Note that this is equivalent to the basic Green's function presented in Equation 4a. By integrating Equation 7 from $x_0 = L_1$ to $x_0 = L_2$ along the line source using the integration formula in Gradsteyn and Ryzhik (1994, 113, equation 2.33), the Green's function for the line source (Figure 1b) is

$$X_2 = \frac{1}{2} \left\{ \operatorname{erf}\left(\frac{x-L_1-v'(t-t_0)}{\sqrt{4D'_{xx}(t-t_0)}}\right) - \operatorname{erf}\left(\frac{x-L_2-v'(t-t_0)}{\sqrt{4D'_{xx}(t-t_0)}}\right) \right\} \exp[-\lambda(t-t_0)] \quad (8)$$

where L_1 is the x coordinate of the beginning of the source and L_2 the x coordinate of the end of the line source.

y Direction

There are six Green's functions available in AT123D-AT for dispersive transport in the y direction. Two of the functions represent solutions for transport in an infinite width aquifer and four represent solutions for transport in a finite-width aquifer. The Green's function for dispersive transport in the y direction, from a point source in an aquifer of infinite width is

$$Y_1 = \frac{1}{\sqrt{4\pi D'_{xx}(t-t_0)}} \exp\left[-\frac{(y-y_0)^2}{4D'_{yy}(t-t_0)}\right] \quad (9)$$

where y_0 is the y coordinate of the point source. Note that this is equivalent to the basic Green's function presented in Equation 4b. By spatially integrating the point source in Equation 9 over the length of the line source from $y_0 = B_1$ to $y_0 = B_2$, the Green's function for dispersive transport in the y direction from a line source (Figure 1c) in an aquifer of infinite width is

$$Y_2 = \frac{1}{2} \left\{ \operatorname{erf}\left(\frac{y-B_1}{\sqrt{4D'_{yy}(t-t_0)}}\right) - \operatorname{erf}\left(\frac{y-B_2}{\sqrt{4D'_{yy}(t-t_0)}}\right) \right\} \quad (10)$$

where B_1 is the y coordinate of the beginning of the line source and B_2 the y coordinate of the end of the line source.

The two solution options for dispersive transport in the y direction from point sources in a finite-width aquifer are

$$Y_3 = \frac{1}{B} + \frac{2}{B} \sum_{m=1}^{\infty} \cos\left(\frac{m\pi y}{B}\right) \cdot \cos\left(\frac{m\pi y_0}{B}\right) \times \exp\left[-\left(\frac{m\pi}{B}\right)^2 D'_{yy}(t-t_0)\right] \quad (11a)$$

$$Y_4 = \frac{1}{\sqrt{4\pi D'_{yy}(t-t_0)}} \times \left\{ \sum_{m=-\infty}^{\infty} \exp\left[-\frac{\{2mB - (y+y_0)\}^2}{4D'_{yy}(t-t_0)}\right] + \sum_{m=-\infty}^{\infty} \exp\left[-\frac{\{2mB - (y-y_0)\}^2}{4D'_{yy}(t-t_0)}\right] \right\} \quad (11b)$$

where m is a summation subscript and B the width of the aquifer. Function Y_3 is an eigenfunction expansion (Carslaw and Jaeger 1959, 361, equation 7) and Y_4 is a solution based on the method of images (Haberman 1987, 414, equation 10.3.25) where the point-source solution is reflected about $y = 0$ and $y = B$ to produce no-flux boundary conditions at the lateral edges of the aquifer. AT123D-AT utilizes function Y_3 when $D'_{yy}(t-t_0)/B^2 \geq 1$ and Y_4 when $D'_{yy}(t-t_0)/B^2 \leq 1$ in order to improve the overall convergence rate for different combinations of parameter values that are used.

By spatially integrating the point-source solutions in Equations 11a and 11b over the length of the line source from $y_0 = B_1$ to $y_0 = B_2$, the two solution options available in AT123D-AT for dispersive transport in the y direction from a line source (Figure 1c) in an aquifer of finite width are, respectively:

$$Y_5 = \frac{B_2 - B_1}{B} + \frac{2}{B} \sum_{m=-\infty}^{\infty} \cos\left(\frac{m\pi y}{B}\right) \cdot \frac{B}{m\pi} \times \left\{ \sin\left(\frac{m\pi B_2}{B}\right) - \sin\left(\frac{m\pi B_1}{B}\right) \right\} \cdot \exp\left[-\left(\frac{m\pi}{B}\right)^2 D'_{yy}(t-t_0)\right] \quad (12a)$$

$$Y_6 = \frac{1}{2} \sum_{m=-\infty}^{\infty} \left[\operatorname{erf}\left[\frac{2mB + (y-B_1)}{\sqrt{4D'_{yy}(t-t_0)}}\right] - \operatorname{erf}\left[\frac{2mB + (y-B_2)}{\sqrt{4D'_{yy}(t-t_0)}}\right] + \operatorname{erf}\left[\frac{2mB - (y+B_1)}{\sqrt{4D'_{yy}(t-t_0)}}\right] - \operatorname{erf}\left[\frac{2mB - (y+B_2)}{\sqrt{4D'_{yy}(t-t_0)}}\right] \right] \quad (12b)$$

where function Y_5 is an eigenfunction expansion and Y_6 a solution based on the method of images. As with functions Y_3 and Y_4 , AT123D-AT utilizes function Y_5 when $D'_{yy}(t-t_0)/B^2 \geq 1$, and Y_6 when $D'_{yy}(t-t_0)/B^2 \leq 1$ in order to improve the convergence rate.

z Direction

There are also six Green's functions available in AT123D-AT for dispersive transport perpendicular to flow in the z direction. Two of the functions represent solutions for transport in an infinite-width aquifer and four represent new solutions in AT123D-AT for transport in a finite-depth aquifer. The solution for dispersive transport in the z direction from a point source in an aquifer of infinite depth is

$$Z_1 = \frac{1}{\sqrt{4\pi D'_{zz}(t-t_0)}} \left\{ \exp\left[-\frac{(z-z_0)^2}{4D'_{zz}(t-t_0)}\right] + \exp\left[-\frac{(z+z_0)^2}{4D'_{zz}(t-t_0)}\right] \right\} \quad (13)$$

where z_0 is the z coordinate of the point source. The first exponential term in Equation 13 is analogous to Equation 4c but Equation 13 also contains an image term to generate a no-flux boundary at the top of the aquifer ($z = 0$). By integrating this point-source solution (Equation 13) from $z_0 = H_1$ to $z_0 = H_2$ along the line source, the solution for dispersive transport in the z direction from a line source

(Figure 1d) in an aquifer of infinite depth is

$$Z_2 = \frac{1}{2} \left[\operatorname{erf} \left[\frac{z - H_1}{\sqrt{4D'_{zz}(t - t_0)}} \right] - \operatorname{erf} \left[\frac{z - H_2}{\sqrt{4D'_{zz}(t - t_0)}} \right] \right. \\ \left. - \operatorname{erf} \left[\frac{z + H_1}{\sqrt{4D'_{zz}(t - t_0)}} \right] + \operatorname{erf} \left[\frac{z + H_2}{\sqrt{4D'_{zz}(t - t_0)}} \right] \right] \quad (14)$$

where H_1 is the z coordinate of the beginning of the line source and H_2 the z coordinate of the end of the line source.

The two solutions in AT123D-AT for dispersive transport in the z direction from a point source in a finite-depth aquifer are

$$Z_3 = \frac{1}{H} + \frac{2}{H} \sum_{m=1}^{\infty} \cos \left(\frac{m\pi z}{H} \right) \cdot \cos \left(\frac{m\pi z_s}{H} \right) \\ \times \exp \left[- \left(\frac{m\pi}{H} \right)^2 D'_{zz}(t - t_0) \right] \quad (15a)$$

$$Z_4 = \frac{1}{\sqrt{4\pi D'_{zz}(t - t_0)}} \\ \times \left\{ \sum_{m=-\infty}^{\infty} \exp \left[- \frac{\{-2mH + (z - z_s)\}^2}{4D'_{zz}(t - t_0)} \right] \right. \\ \left. + \sum_{m=-\infty}^{\infty} \exp \left[- \frac{\{-2mH + (z + z_s)\}^2}{4D'_{zz}(t - t_0)} \right] \right\} \quad (15b)$$

where H is the saturated thickness of the aquifer, and $(t - t_0)$ is the time elapsed since the time the instantaneous point-source release is applied at the location z_0 . Function Z_3 is an eigenfunction expansion (Carslaw and Jaeger 1959, 361, equation 7) and Z_4 is a new solution based on the method of images (Haberman 1987, 414, equation 10.3.25) where the point-source solution is reflected about $z = 0$ and $z = H$ to produce no-flux boundary conditions at the top and bottom of the aquifer. AT123D-AT utilizes function Z_3 when $D'_{zz}(t - t_0)/H^2 \geq 1$ and Z_4 when $D'_{zz}(t - t_0)/H^2 \leq 1$ to improve the convergence rates of these series solutions.

By integrating Equations 15a and 15b from $z_0 = H_1$ to $z_0 = H_2$, the two new solutions for a line source available in AT123D-AT for dispersive transport in the z direction from a line source (Figure 1d) in an aquifer of finite depth are respectively:

$$Z_5 = \frac{H_2 - H_1}{H} + \frac{2}{H} \sum_{m=1}^{\infty} \cos \left(\frac{m\pi z}{H} \right) \\ \cdot \frac{H}{m\pi} \left\{ \sin \left(\frac{m\pi H_2}{H} \right) - \sin \left(\frac{m\pi H_1}{H} \right) \right\} \\ \cdot \exp \left[- \left(\frac{m\pi}{H} \right)^2 D'_{zz}(t - t_0) \right] \quad (16a)$$

$$Z_6 = \frac{1}{2} \sum_{m=-\infty}^{\infty} \operatorname{erf} \left[\frac{2mH + (z - H_1)}{\sqrt{4D'_{zz}(t - t_0)}} \right] \\ - \operatorname{erf} \left[\frac{2mH + (z - H_2)}{\sqrt{4D'_{zz}(t - t_0)}} \right] + \operatorname{erf} \left[\frac{2mH + (z + H_1)}{\sqrt{4D'_{zz}(t - t_0)}} \right] \\ - \operatorname{erf} \left[\frac{2mH + (z + H_2)}{\sqrt{4D'_{zz}(t - t_0)}} \right] \quad (16b)$$

where function Z_5 is an eigenfunction expansion and Z_6 is a solution based on the method of images. As before, AT123D-AT utilizes function Z_5 when $D'_{zz}(t - t_0)/H^2 \geq 1$ and Z_6 when $D'_{zz}(t - t_0)/H^2 \leq 1$ in order to improve the convergence rate of the series solutions.

Source Representation Methods

In order to approximate the effects of mass entering the aquifer via leachate from the vadose zone, a landfill, or leakage from an overlying aquifer/aquitard system, one approach is to use a horizontal planar source located at the top of the aquifer ($z = 0$) with the area of the rectangular plane approximating the distribution of mass in the zone above. Although this approach is relatively easy to implement, it has the disadvantage of understating the amount of mixing going on directly below the source. The solution will account for the effects of dispersion below the source, but not for the influence of vertical advection due to the water infiltration from above, that is, no volumetric water sources are assumed in the model. At some distance from the source, the effects of neglecting the influence of vertical advection are usually negligible, but near the source, the influence may be noticeable with the model generating near-source concentrations that are greater than the source leachate concentrations assumed to enter the system. These seemingly anomalous results are a function of the nature of the mass-loading source term. Resultant near-source concentrations are based on: (1) mass mixing with the quantity of water passing through a vertical rectangular plane defined by the source width and thickness (zero for the case above) and (2) the influence of vertical dispersion directly below the source.

This near-source over-estimate of concentration often can be circumvented by representing the source as a rectangular prism with $H_1 = 0$ and the source of thickness $H_2 = T_{\text{source}}$ in AT123D-AT. A simple way to approximate the source thickness is to assume that:

$$T_{\text{source}} = \frac{I_f L_{\text{source}}}{q} \quad (17)$$

where L_{source} is the source length in the direction of flow, I_f is the infiltration rate, and q is the Darcy velocity of the aquifer. A more accurate calculation for source thickness that takes into consideration the change of vertical velocity with depth is (Electric Power Research

Institute [EPRI] 1993, equation 59):

$$T_{\text{source}} = H \left(1 - \exp \left[-\frac{I_f L_{\text{source}}}{Hq} \right] \right). \quad (18)$$

The equation for source thickness (source penetration depth), as presented in EPRI (1993), also contains a term for vertical dispersion. The dispersive term should not be used with AT123D or AT123D-AT because the influence of vertical dispersion beneath the source is already represented in its analytical solutions that are infinite in the direction of flow. The plume depth term with dispersion included is only valid for solutions that are semi-infinite in the flow direction with the finite upgradient edge of the system defined by a vertical planar source that begins at the downgradient edge of the source area (i.e., a landfill). Both Equations 17 and 18 give similar results when $T_{\text{source}} \ll H$.

Updated Numerical Integration Scheme

A major difference between AT123D and AT123D-AT is the manner in which the time integrals in the solutions are evaluated numerically. The original version of AT123D uses a composite Simpson's rule integration formula (Carnahan et al. 1969; Conte and de Boor 1980). In a composite integration rule, the interval of integration is subdivided in smaller intervals and then the formula is used separately in each subinterval. In AT123D, a constant time-step (subinterval of integration) length is chosen, and the model solves for unknown values at a series of gridded points. The inherent weakness to this integration scheme is that the accuracy of the solution is dependent on the size of the time step. The size of the time step needed to produce an accurate answer is dependent upon the location of the point of evaluation and the time at which the solution is sought. At a grid of observation points, for all points to be evaluated correctly, the appropriate time step in AT123D is controlled by points near the source where transient concentration changes are more rapid. The small time step needed to derive an accurate solution for an observation point near the source may lead to the need for a prohibitively large number of time steps to evaluate downgradient points. To ensure an accurate answer, repeated simulations with different time steps are required.

In addition, the original AT123D can have inaccurate quasi-oscillatory numerical errors in the solution between alternating odd- and even-numbered time steps. The composite Simpson's rule, as utilized in AT123D, dictates the need for an odd number of integrand calculation points (Conte and de Boor 1980, 321). For generation of results with an even number of integrand calculation points, AT123D uses the trapezoidal rule for evaluating the last subinterval. For transient sources, the lower accuracy of the trapezoidal rule can cause the results to artificially oscillate over time when the selected time steps are too large.

To circumvent the occurrence of problems associated with the numerical integration technique in AT123D, the scheme implemented in AT123D-AT uses a composite trapezoidal with an interval refinement algorithm and a Romberg algorithm with extrapolation. The composite trapezoidal with refinement algorithm uses trapezoidal rule integration over successive refinements of subintervals until a desired degree of accuracy is obtained. This type of algorithm is robust and can be used to evaluate the integrals of functions that are not smooth (Conte and de Boor 1980; Press et al. 1992). The Romberg algorithm with extrapolation represents a more efficient algorithm that works well with steady or pulse sources.

For time-variant sources, the optimal integration technique is a function of the nature of the source. If the time-variant source is a well behaved smooth function (i.e., non-oscillatory), the Romberg method will work and will be the most efficient option. If the source fluctuates over time, the composite trapezoidal with refinement algorithm is preferable. A third option, based upon the time intervals used to describe the time-variant source term, also is provided in AT123D-AT. This option breaks the integral up into subintegrals, based upon the time intervals. Each subintegral is evaluated through a choice of using either the composite trapezoidal with refinement algorithm or the Romberg extrapolation method. This choice is useful when the time series shows a high-frequency oscillatory type behavior. The use of subintegrals is inefficient for a smooth function. All the integration options included in AT123D-AT check for convergence based on a predetermined error criteria.

Improvements in Computational Efficiency

The use of numerical integration to evaluate simulation results for long time periods can have not only computational errors but also excessive computer run times. This is especially of concern in a code like AT123D-AT where the solution is desired for a grid of points where steady results may be reached almost instantaneously for some points while other points may need hundreds of years or more to reach a steady concentration. Non-convergence-testing methods, similar to those in AT123D, are efficient but may provide incorrect answers. If not limited in the number of integral partitions allowed, convergence-testing methods such as the composite trapezoidal with refinement algorithm provide the correct solution but can take excessively long computation times.

AT123D-AT includes code improvements for both increasing computational accuracy and reducing the computer run time. If a preset limit to the number of partitions allowed is reached, the code will pause and a warning message is given. If necessary, the allowable number of partitions in the integration subroutines can then be increased to improve accuracy. In order to improve computational efficiency during numerical integration, AT123D-AT will check for approximate steady-state conditions based on a prespecified concentration

change criterion, and the code will stop solving at individual analysis points when the steady-state criterion is met. The output for these points then becomes the last solved-for solution until the simulation is finished. As individual points reach the denoted change-over-time criteria, they are dropped from the solution scheme and the analysis continues until all points reach a “steady” solution. For pulse-source solutions, the same method is applied, but the simulation itself continues. After the time the pulse is turned off, the code once again actively starts solving at each point. A similar solution turn-off logic is applied after the pulse-off time is reached. After an individual point has reached its maximum concentration, the solution is turned off when a prespecified very low value is reached in the concentration change between successive time steps.

Finite-Duration (Pulse) Source Release Example

To test the code modifications in AT123D-AT, a 3D model was used to simulate conservative contaminant transport from a pulse-source release at a constant rate. A rectangular prismatic source (Figure 2b) was used in an aquifer with infinite width and finite thickness of 25 m. The model parameters are summarized in Table 1. The source was applied from $t = 0$ to $t = 150$ days and then was turned off. The analytical solution for this problem is:

$$\begin{aligned}
 C(x, y, z, t) &= \frac{\dot{M}}{n_e R} \int_0^t F_{22k}(x, y, z, t; t_0) dt_0 \\
 &= \frac{\dot{M}}{n_e R} \int_0^t X_2 Y_2 Z_k dt_0 \quad t < T \\
 &= \frac{\dot{M}}{n_e R} \int_0^T F_{22k}(x, y, z, t; t_0) dt_0 \\
 &= \frac{\dot{M}}{n_e R} \int_0^t X_2 Y_2 Z_k dt_0 \quad t > T \quad (19)
 \end{aligned}$$

where $k = 5$ (Equation 16a) is used for Z_k when $D'_{zz}(t - t_0)/H^2 \geq 1$ or $k = 6$ (Equation 16b) is used for Z_k when $D'_{zz}(t - t_0)/H^2 \leq 1$ for this finite-depth Green's function with X_2 and Y_2 given by Equations 8 and 10, respectively. Because Z_k is an infinite series in Equation 19, the integrals cannot be evaluated analytically and must be calculated numerically. For this example, Romberg algorithm with extrapolation was used in AT123D-AT.

This simulation was performed for a total time of 300 d, and the breakthrough curve at $x = 202.5$ m, $y = 0$ m, and $z = 0$ m was examined. During the initial code testing, the results of the AT123D-AT simulation were compared with the results from AT123D, but did not match. To determine the source of this discrepancy, the simulated concentration results generated using the pulse-source options (C_{pulse}) in AT123D-AT and AT123D were compared to the simulated concentration results generated

Table 1
AT123D-AT Model Parameter Values

Half-Source release rate: 6.28 g/d
Source length x coordinates: $L_1 = 120$ m to $L_2 = 150$ m
Half-source width y coordinates: $B_1 = 0$ m to $B_2 = 15$ m
Source depth z coordinates: $H_1 = 0$ m to $H_2 = 2.5$ m
Darcy groundwater flow rate (q): 0.25 m/d
Effective porosity (n_e): 0.25
Longitudinal dispersivity (a_{xx}): 30 m
Horizontal transverse dispersivity (a_{yy}): 15 m
Vertical transverse dispersivity (a_{zz}): 2.5 m
Retardation factor: 1
Degradation rate constant (λ): 0 d ⁻¹
Aquifer thickness (H): 25 m
Pulse release duration: $T = 150$ d
Total simulation time: 300 d

using the steady-source option (C_{steady}) in AT123D, and taking advantage of the principle of superposition:

$$C_{\text{pulse}}(x, y, z, t) = C_{\text{steady}}(x, y, z, t) \quad (20)$$

when $t \leq t_{\text{pulse}}$,

$$\begin{aligned}
 C_{\text{pulse}}(x, y, z, t) &= C_{\text{pulse}}(x, y, z, t) \\
 &- C_{\text{steady}}(x, y, z, t - t_{\text{pulse}}) \quad \text{when } t > t_{\text{pulse}} \quad (21)
 \end{aligned}$$

where t_{pulse} is the time the pulse ends. As can be seen in Figure 3, the results generated using AT123D-AT match the results generated using the AT123D steady-source option and superimposing the results of the steady-source simulation with the appropriate time shift. The results generated by AT123D using the pulse-source option did not match the expected value. A closer examination of the original version of AT123D showed that the numerical integration scheme was incorrectly coded for the pulse-source option.

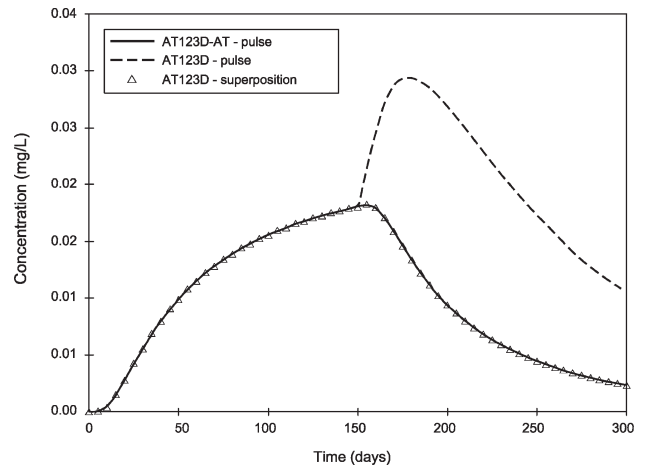


Figure 3. Comparison of simulated concentration vs. time using AT123D-AT and AT123D for a pulse-source problem at $x = 202.5$ m, $y = 0$ m, and $z = 0$ m.

Numerical Model Code Comparison Example

As a test of the implementation of the updated time-integration scheme and both the aquifer finite-width and finite-depth series approximations in AT123D-AT, a problem considering fully 3D transport from a rectangular prismatic source, was simulated and compared to results from the 3D finite-difference model MODFLOWT (Duffield and GeoTrans 1996). In this simulation, the aquifer width (B) is assumed to be 300 m. In addition, the source mass flux is assumed to be constant for the entire simulation. The source dimensions and other model parameters are the same as in the previous example and are given in Table 1. The analytical solution for the concentration at location (x, y, z) at time t is

$$C(x, y, z, t) = \frac{\dot{M}}{n_e R} \int_0^t F_{2jk}(x, y, z, t; t_0) dt_0$$

$$= \frac{\dot{M}}{n_e R} \int_0^t X_2 Y_j Z_k dt_0 \quad (22)$$

where $j = 5$ (Equation 12a) is used for Y_j when $D'_{yy}(t - t_0)/B^2 \geq 1$ or $j = 6$ (Equation 12b) is used for Y_j when $D'_{yy}(t - t_0)/B^2 \leq 1$, $k = 5$ (Equation 16a) is used for Z_k when $D'_{zz}(t - t_0)/H^2 \geq 1$ or $k = 6$ (Equation 16b) is used for Z_k when $D'_{zz}(t - t_0)/H^2 \leq 1$, and X_2 is given by Equation 8. Because Y_j and Z_k are infinite series in Equation 22, the integral cannot be evaluated analytically and must be calculated numerically. For this example, Romberg algorithm with extrapolation was used in AT123D-AT.

For the MODFLOWT simulation, the finite-difference grid was discretized into a rectangular grid of 102 blocks in the flow direction (x direction), 30 blocks in the y direction, and 28 blocks in the z direction. The input for both models was designed to take advantage of the symmetry of the problem by simulating half of the volume across the centerline of the source in the y direction. The grid spacing was constant and set to $\Delta x = 5$ m and $\Delta y = 5$ m in the horizontal plane. For the vertical discretization, the grid spacing was set to $\Delta z = 0.5$ m at source level and $\Delta z = 1.0$ m throughout the rest of the depth (except for two transition blocks of thickness $\Delta z = 0.75$ m under the source-level blocks). The upgradient boundary nodes were simulated as zero-concentration Dirichlet (constant concentration nodes). The lateral, bottom, and downgradient boundary conditions were of Neuman type (no-flux). In MODFLOWT, the source was simulated by partitioning the mass flux equally among the 90 blocks within the rectangular prismatic source area. The source was located in a region along the x axis at $x = 120$ m to $x = 150$ m from the upgradient edge of the model, from $y = 0$ and $y = 15$ m, and from the top of the system $z = 0$ to a depth of $z = 2.5$ m.

Figure 4 shows the results at a depth of 1.25 m for an early time of 30 d and a late time of 300 d. As shown in this figure, the early time results are very similar (Figure 4a). A comparison of the results at late time (Figure 4b) shows very similar results except at the

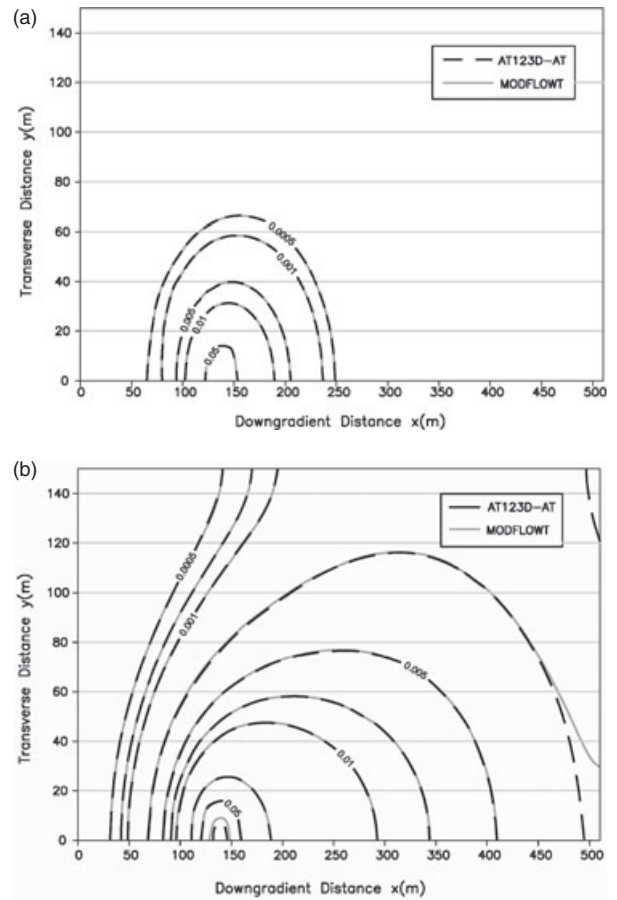


Figure 4. Comparison between AT123D-AT and MODFLOWT results for three-dimensional transport at a depth of 1.25 m after: (a) 30 d and (b) 300 d.

downgradient boundary. The difference in results is a function of the different boundary conditions for the governing equations used by AT123D-AT and MODFLOWT. As stated above, MODFLOWT utilized a Neuman type ($\partial C/\partial x = 0$) at the downgradient edge, and its effect is seen when the plume reaches the model boundary as shown for the time of 300 d in Figure 4b. This effect is not seen in the AT123D-AT results because its boundary conditions are specified at infinity in the x direction of groundwater flow.

Conclusions

The use of Green's functions in semi-analytical codes such as AT123D is a versatile tool to examine the fate and transport of dissolved chemicals, radionuclides, and heat in groundwater for a variety of source configurations and mass flux changes over time. Because AT123D applications can have difficulties in generating correct answers, a new version, AT123D-AT, was developed to facilitate the generation of accurate solutions. In particular, the numerical evaluation of the analytical solutions is now performed in a manner that generates accurate solutions regardless of time steps and evaluation points that are chosen. In addition, the computational efficiency of the code

was improved by eliminating calculations at points during numerical integration where the solution has reached approximate steady state. Updated series solution approximations were included in order to improve convergence rates for finite-depth aquifers. AT123D-AT also includes code modifications to correctly simulate transport of dissolved constituents for the case of a pulse source, which was not accurately simulated using the original AT123D.

Software Availability

The AT123D-AT program code is written in FORTRAN-90 and many of its modifications are discussed by USEPA (1997), and in the user's guide (Lester and Burnell 2011). This updated version (AT123D-AT) includes corrections for known errors inherent to other versions of AT123D and improved model output formatting to facilitate generation of areal and time series plots. Upon written request, the source code, compiled executable, and user's guide that gives detailed examples of its use may be obtained from the authors or Integrated Groundwater Modeling Center (IGWMC) without charge.

Acknowledgments

This work was funded by the U.S. EPA National Risk Management Laboratory and Tetra Tech GEO research and development. We thank Dr. David Burden, director of the Technical Support Center of the Ground Water and Ecosystems Restoration Division (GWERD), for his interest, support, and guidance. The authors also wish to thank the anonymous reviewers for their technical review and insightful comments, which helped to strengthen and improve this manuscript. Appreciation is also expressed to Joanne Rose and Christina Paugh for their time spent working on the manuscript and graphics.

References

- American Petroleum Institute (API). 1994. Decision support system for exposure and risk assessment. User's Guide Version 1.0.
- Aziz, C.E., C.J. Newell, J.R. Gonzales, P.E. Haas, T.P. Clement, and Y. Sun. 2000. BIOCHLOR natural attenuation decision support system. User's Manual Version 1.1. Washington, DC: U.S. EPA Office of Research and Development, EPA/600/R-00/008.
- Bonazountas, M., and J.M. Wagner. 1984. SESOIL: A seasonal soil compartment model. Cambridge MA: Arthur D. Little, Inc. Prepared for U.S. EPA Office of Toxic Substances. National Technical Information Service publication PB86-112406.
- Burnell, D.K., J.W. Mercer, and L.S. Sims. 2011. Analytical models of steady-state plumes undergoing Sequential Degradation. *Ground Water*. DOI: 10.1111/j.1745-6584.2011.00858.x.
- Carnahan, B., H.A. Luther, and J.O. Wilkes, 1969. *Applied Numerical Methods*. New York: John Wiley & Sons.
- Carslaw, H.S., and J.C. Jaeger. 1959. *Conduction of Heat in Solids*. 2nd ed. Oxford: Clarendon Press.
- Conte, S.D., and C. de Boor. 1980. *Elementary Numerical Analysis*. 3rd ed. New York: McGraw-Hill.
- Cecan, L., and R. Schneiber. 2010. BIOSCREEN, AT123D and MODFLOW/MT3D: A comprehensive review of model results. *International Journal of Soil, Sediment, and Water* 3, no. 2: 1-18.
- Domenico, P.A. 1987. An analytical model for multidimensional transport of a decaying contaminant species. *Journal of Hydrology* 91, 49-58.
- Duffield, G.M., and GeoTrans. 1996. MODFLOWT: A Modular Three-Dimensional Groundwater Flow and Transport Model, *User's Guide* Version 1.1.
- Electric Power Research Institute (EPRI). 1993. ROAM™ remedial options assessment model. User's Guide Version 1, EPRI TR-103202.
- Environmental Consultants Inc. 2006. SEVIEW: integrated contaminant fate and transport modeling system. User's Guide Version 6.3, January 2006.
- General Sciences Corporation. 1995. RiskPro's seasonal soil compartment model (SESOIL) for windows. User's Guide for January 1995 version. Prepared for U.S. EPA, OTS, Contract No. 68-02-4281.
- Gradshteyn, I.S., and I.M. Ryzhik. 1994. *Table of Integrals, Series, and Products*, 5th ed., 1204. New York: Academic Press.
- Haberman, R. 1987. *Elementary Applied Partial Differential Equations with Fourier Series and Boundary Value Problems*, 2nd ed. Englewood Cliffs, New Jersey: Prentice-Hall.
- Hetrick, D.M., S.J. Scott, and M.J. Barden. 1993. *The New Sesoil User's Guide*, prepared for the Wisconsin Department of Natural Resources, Emergency and Remedial Response Section, Bureau of Solid and Hazardous Waste Management, Madison, Wisconsin.
- Hetrick, D.M., C.C. Travis, S.K. Leonard, and R.S. Kinerson. 1989. Qualitative validation of pollutant transport components of an unsaturated soil zone model (SESOIL), ORNL/TM-10672, Oak Ridge National Laboratory, Oak Ridge, Tennessee.
- Jury, W.A., D. Russo, G. Streile, and H. El Abd. 1990. Evaluation of organic chemicals residing below the soil surface. *Water Resources Research* 26, no. 1: 13-20.
- Kellogg, O.D. 1955. *Foundations of Potential Theory*, New York: Dover.
- King, K.S., and P. Geo. 2006. Hydrogeologic assessment tools to determine the rate of biodegradation of contaminants in groundwater. February 2006 report submitted to Scientific Advisory Board for Contaminated Sites, British Columbia, Canada.
- Lester, B.H., and D.K. Burnell. 2011. AT123D-AT: Documentation and User's Guide, Version 2.0, Tetra Tech GEO, Inc. <http://www.tetrattechgeo.com/publicatons.html> (accessed December 5, 2011).
- New Jersey Department of Environmental Protection (NJDEP). 2008. Guidance for using the SESOIL and AT123D models to develop site specific impact to ground water soil remediation standards. June 2, 2008.
- Newell, C.J., R.K. McLeod, and J. Gonzales. 1996. BIOSCREEN Natural Attenuation Decision Support System. U.S. Environmental Protection Agency, EPA/600/R-96/087 (August).
- Odencrantz, J.E., J.M. Farr, and C.E. Robinson. 1992. Transport model sensitivity for soil cleanup level determinations using SESOIL and AT123D in the context of the California Leaking Underground Fuel Tank Field Manual. *Journal of Soil Contamination* 1, no. 2: 159-182.
- Press, W.H., S.A. Teukolsky, W.T. Vetterling, and B.P. Flannery. 1992. *Numerical Recipes in FORTRAN, The Art of Scientific Computing*. 2nd ed. New York: Cambridge University Press.
- Sinton, L.W., M.J. Noonan, R.K. Finlay, L. Pang, and M.E. Close. 2000. Transport and attenuation of bacteria and bacteriophages in an alluvial gravel aquifer. *New Zealand Journal of Marine and Freshwater Research* 24, no. 1: 20-25.

- Srinivasan, V., T.P. Clement, and K.K. Lee. 2007. Domenico solution—Is it valid? *Groundwater* 45, no. 2: 136–148.
- USEPA. 1997. AT123D97: Documentation and user's guide. Robert S. Kerr Environmental Research Laboratory Center for Subsurface Modeling Support, Version 1.0 (Draft), Ada, Oklahoma.
- USEPA. 1996. VLEACH: A one-dimensional finite difference vadose zone leaching model. Robert S. Kerr Environmental Research Laboratory Center for Subsurface Modeling Support, Version 2.2a, Ada, Oklahoma.
- Water Resources Control Board (WRCB). 1989. Leaking underground fuel tank (LUFT) field manual: guidelines for site assessment, cleanup, and underground storage tank closure. Sacramento, California: Leaking Underground Fuel Tank Task Force.
- West, M.R., B.H. Kueper, and M.J. Unga. 2007. On the use and error of approximation in the Domenico (1987) solution. *Ground Water* 45, no. 2: 126–135.
- Yeh, G.T. 1993. AT123D: Analytical transient one-, two-, and three-dimensional simulation of waste transport in the aquifer system. IGWMC Ground Water Modeling Software. International Ground Water Modeling Center, IGWMC-FOS 38 PC, Version 1.22.
- Yeh, G.T. 1981. AT123D: Analytical transient one-, two-, and three-dimensional simulation of waste transport in the aquifer system. ORNL-5602, Oak Ridge National Laboratory, Oak Ridge, Tennessee.